

Laminar burning velocities of propene–air mixtures at elevated temperatures and pressures

K. Saeed¹ and R. Stone*²

Propene (C₃H₆) is a key intermediate species in the combustion of higher alkanes and alkenes, yet the only significant published data since the 1950s appear to be for the laminar burning of propene–air mixtures at close to ambient conditions. The work undertaken here has generated data for the burning velocities of the propene–air mixtures at varying temperatures and pressures in a constant volume spherical vessel with central ignition. A multiple burned gas zone model has been used to give the relationship between the pressure rise and mass fraction burned. The initial temperatures were 293 and 425 K, with initial pressures of 0.5, 1.0, 2.0, 3.5 bar, and equivalence ratios of 0.8 to 1.6, from which data have been obtained for the laminar burning velocity at pressures up to 20 bar and unburned gas temperatures up to 650 K. The data have been fitted to a nine term equation to describe the effects of: stoichiometry, pressure, and temperature. Burning velocity data for propene–air mixtures have been compared with earlier reported data, and the values obtained from the present study are in very good agreement with the data of Davis and Law for ambient conditions. Cellular flames were found to exist in some test runs and the conditions of the cellularity onset are reported.

Keywords: Multizone model, Burning velocity, Propene–air

List of symbols

A	inside surface area of the vessel
B	inside diameter of the vessel
c_p	specific heat
e	specific internal energy
E	internal energy
h	specific enthalpy
h	heat transfer coefficient
K	stretch rate
Le	Lewis number
m	mass
P	pressure
Q	heat transfer
r	radius
S	entropy
S_u	burning velocity
T	temperature
v	specific volume
V	volume
x	mass fraction burned

Subscripts

b	burned
o, I	initial condition
u	unburned condition
w	wall

Introduction

Laminar burning velocity data are of great significance and play an essential role in determining several important aspects of combustion for both practical and theoretical applications. Flame chemistry is commonly studied by performing computer simulations of laminar, one-dimensional (1D) flames by solving complex chemical kinetic schemes. As the chemical kinetic data in such models are not sufficiently well known for the predictions to be used with confidence, it is more usual to use measured burning velocities to validate these chemical kinetics schemes. The production of accurate experimental data on laminar premixed flames therefore plays a key role in the process of understanding a large range of flames.

Combustion of alkanes larger than methane is a complicated subject owing to the great variety of minor species that can be formed. It has been found that alkenes are formed as an intermediate in the combustion of higher alkanes, such as propane, butane, heptane and isooctane, Glassman¹ and Davis *et al.*² reported that propene (C₃H₆) is a key intermediate in the combustion

¹School of Engineering, University of Brighton, Lewes Road, Brighton, BN2 4GJ, UK

²Department of Engineering Sciences, Oxford University, Parks Road, Oxford, OX1 3PJ, UK

*Corresponding author, email Richard.stone@eng.ox.ac.uk

of higher alkanes, such as propane, butane, heptane and iso-octane as these hydrocarbon compounds constitute a notable part of practical hydrocarbon fuels, yet the only published data since the 1950s appear to be for the laminar burning of propene-air mixtures at ambient conditions by Davis and Law³ and Jomaas *et al.*,⁴ who present data at 1, 2 and 5 atm. Data on the burning velocities of propene have been reported by Gerstein *et al.*,⁵ who measured flame propagation in a tube, and Gibbs and Calcote,⁶ who used a burner. The accuracy of these data needs to be questioned, because of complications associated with the determination of the burning velocities using these methods. In the burner method used by Gerstein *et al.*,⁵ a premixed combustible mixture is allowed to flow through a tube and at the end of the tube a conical flame is produced, which is stabilised by the flow of the combustible mixture balancing the rate of consumption of it at the flame front. The burning velocity is calculated by means of the measurement of the conical flame area and mixture flow speed. The apparent simplicity of the method is unfortunately offset by well known shortcomings, such as the effects of flame stretch coupled with mixture diffusion and heat transfer. In the tube method used by Gibbs and Calcote,⁶ a long cylindrical or rectangular tube is filled with a quiescent combustible mixture. The mixture is ignited at one end of the tube; it is closed at other end. A flame front is then established which moves up the tube. The burning velocity is determined from the product of the ratio of tube to flame area and flame front speed. However, in the tube method, a plane propagating flame is unstable and variable, so it is difficult to calculate its area and its flame speed, and hence both are subject to experimental errors. Also, the walls of the tube act as a sink for the removal of heat, thereby reducing the flame velocity at the walls. Davis and Law³ determined the burning velocities of alkenes using a counterflow flame configuration over a range of equivalence ratios at ambient temperature and pressure, and these data from an established technique provide a useful baseline validation for the current study. The counter flow twin flame technique allows the systematic subtraction of an effect called flame stretch from the burning velocity. The experiment involves the establishment of two symmetrical, planar, nearly adiabatic flames in a nozzle generated counter flow. The determination of the axial velocity profile along the centreline of the flow by using the minimum point of the velocity profile as a reference upstream speed S_L corresponding to the imposed stretch rate, K , which by definition is simply the velocity gradient ahead of it. Thus, by plotting S_L versus K , and extrapolating it to $K=0$, it is possible to obtain the laminar burning velocity at zero stretch.

The counter flow technique is an established technique, but there are difficulties associated with it in properly defining the flow field, and the strain rate profiles. Also, the technique is not readily applicable to the generation of data at elevated temperatures and pressures. The constant volume vessel technique is widely used for the determination of the burning velocity, as from a single test run a wide range of data is obtained at varying (but coupled) temperatures and pressures. Recently, Saeed and Stone^{7,8} have developed a novel multiple burned gas zone model to describe the different aspects of premixed laminar combustion in a

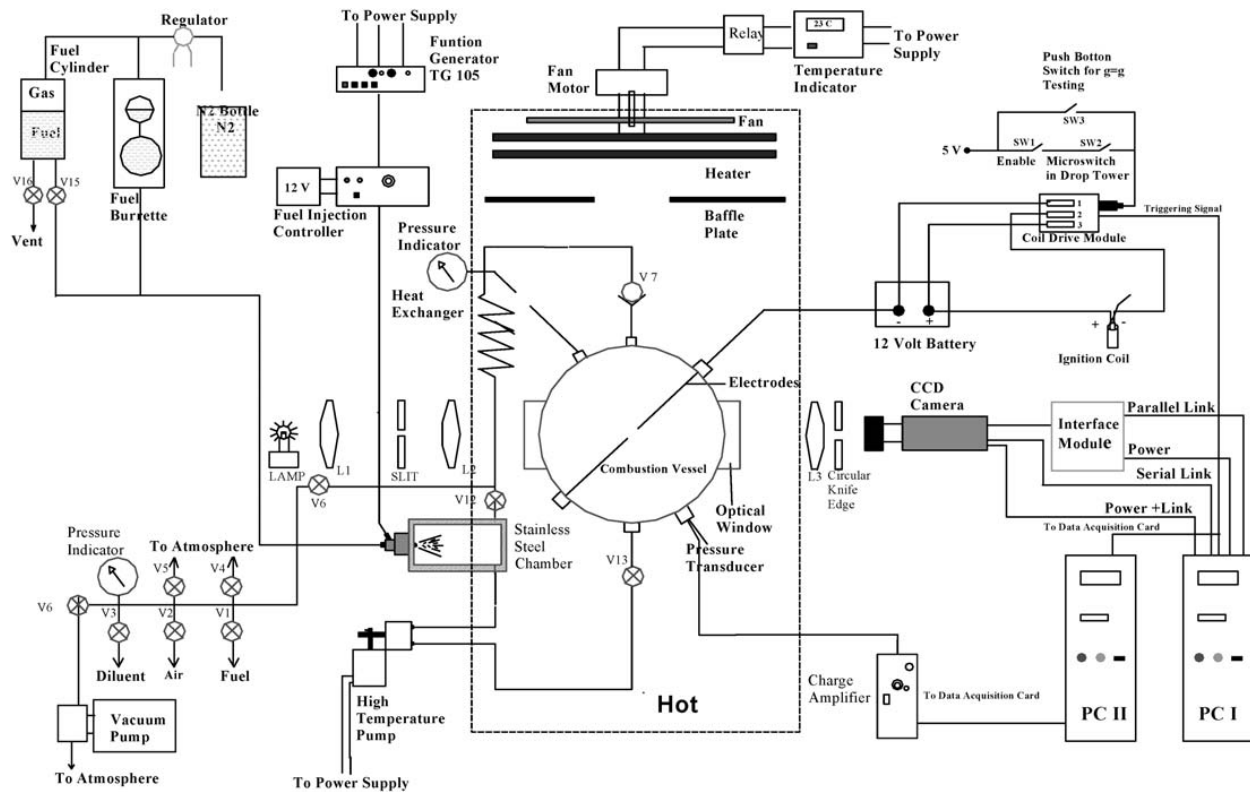
closed spherical vessel and then successfully used it for the determination of the burning velocity. They found that the relationship between the pressure rise and the mass fraction burned is not linear as assumed by Lewis and von Elbe.⁹ The multizone model shows that the error associated with the linear assumption is up to 5%, and the error is a maximum for a stoichiometric mixture. The multizone burning velocity technique is used here to obtain burning velocity data for propene-air mixtures with initial temperatures of 293 and 425 K, initial pressures of 0.5, 1.0, 2.0 and 3.5 bar, and equivalence ratios of 0.8 to 1.6. The burning velocity data for propene-air mixtures are compared with earlier reported data. Cellular flames have been found to exist in some test runs for propene and the conditions of its onset are reported.

Experimental facility and procedures

The experimental facility used in the present work is the same as used by Saeed and Stone.⁸ The test facility (Fig. 1) consists of the following: a combustion vessel and heating system, ignition circuit, gaseous and liquid fuel handling system, and a data acquisition system. The spherical test vessel (160 mm diameter) is provided with central ignition electrodes. The test vessel can withstand a maximum pressure of 34 bar. The combustion vessel is placed inside a heating system, which consists of an oven, made from Sindanyo. The oven is fitted with a fan, temperature controller and air baffle plate. The heating system is employed to achieve two purposes: testing of the mixture at elevated initial temperatures and the evaporation of liquid fuels at high temperatures.

An initial temperature of over 150°C inside the test vessel can be achieved and maintained using the heating system. The combustion vessel is fitted with two diametrically opposed electrodes to achieve central ignition. The electrodes are powered by a standard Lucas inductive ignition system consisting of a coil drive module, two extended equal length electrodes, a 12 V battery, and a switching system for controlling ignition. The ignition system gives a spark energy of ~ 1 mJ (Ref. 10), which is more than the minimum ignition energy of the fuels tested in the present study. Gaseous fuel-air mixtures are prepared by using their partial pressures.

A high temperature circulation pump is connected in series with the steel chamber, combustion vessel and heat exchanger. This ensures homogeneous mixture preparation inside the vessel. Five minutes are allowed for the mixture to become quiescent and homogeneous. This is consistent with the earlier studies of Metghalchi and Keck¹¹ and Clarke¹⁰ as any longer does not make any difference to the burning velocity. A Kistler 701A quartz pressure transducer is used with a Kistler 5001 charge amplifier for the measurement of the dynamic pressure. They were calibrated as a pair using a dead weight tester. A high speed data acquisition system based on Pentium III with a national instrument's data acquisition (DAQ) card is set to record the pressure and ignition signal for the subsequent analysis. The DAQ system consists of a PCI-MIO-16E1 card, which provides 12 bits analogue to digital conversion, a BNC-2090 rack mount, and the LABVIEW programming language for coding the data acquisition 'front panel'. The data sampling rate is set at 25 kHz, and the



1 Representation of experimental facility

dynamic pressure measurement is triggered by the voltage history of the primary circuit of the ignition coil.

The advantage of using the pressure rise to generate laminar burning velocity data is that a single experiment yields data for a wide range of coupled pressures and temperatures, and by varying the initial temperature or pressure, then the pressure/temperature dependency can be decoupled; see for example work of Stone *et al.*¹⁰ The disadvantage of the pressure rise method is that if cellularity occurs, then the data can not be used. However, cellularity can be detected from discontinuities in the laminar burning velocity data (this will be shown later) – discontinuities in the pressure record are not sensitive enough.

A multiple zone model⁸ is used to calculate the relationship between the mass fraction burned and pressure rise, the temperature gradient in the burnt gas, and the thermodynamic properties of the burned and unburned gas, so that the flame radius and burning velocity can be computed. The model assumes a thin flame front separating the burned and unburned gas, an assumption that is also used in many combustion models. This model was successfully used for the determination of the burning velocities in Saeed and Stone.^{7,8} The assumptions and method used for the determination of the burning velocities are the same as used in Saeed and Stone.^{7,8} The burning velocity calculations assume a spherical flame front within a spherical closed vessel filled with homogeneous combustible mixture. At time $t=0$, the mixture is ignited at the centre, a spherical flame front is established instantaneously, and begins to propagate outwardly to reach the wall. Considering an elemental shell of thickness dr_i at radius r_i . If, during the travel of the flame through the vessel, the burned gas had not expanded, then an element dr_i would be the thickness of a shell at the temperature T_i , and pressure P_i

about to be traversed by the wave in the time element dt , as shown in Fig 2a. Its volume would have been

$$4\pi r_i^2 dr_i \quad (1)$$

However, by expansion, the radius of the shell increased from r_i to r_b , the pressure to P and the temperature of the shell to T_u . Therefore, its volume is actually

$$4\pi r_i^2 dr_i \left(\frac{T_u P_i}{T_i P} \right) \quad (2)$$

Since the thickness of the shell is equal to $S_u dt$, its volume is also equal to

$$4\pi r_b^2 S_u dt \quad (3)$$

Equating equations (2) and (3) gives the equation for the burning velocity as

$$S_u = \left(\frac{dr_i}{dt} \right) \left(\frac{r_i}{r_b} \right)^2 \left(\frac{T_u P_i}{T_i P} \right) \quad (4)$$

The unburned gas is assumed to undergo isentropic compression, so its temperature can be calculated by

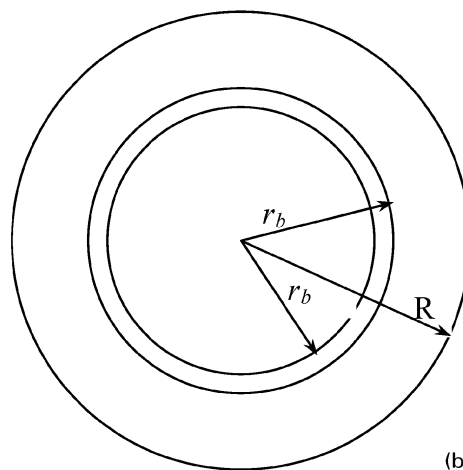
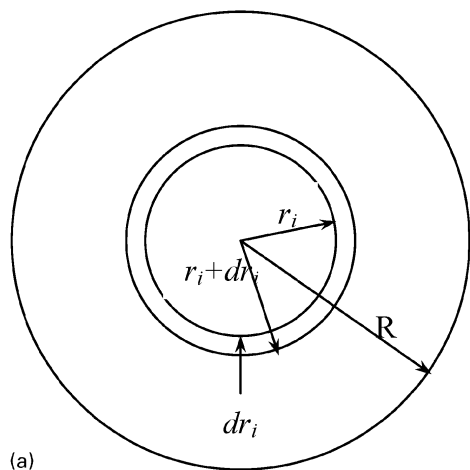
$$T_u = T_i \left(\frac{P}{P_i} \right)^{\frac{\gamma_u - 1}{\gamma_u}} \quad (5)$$

Substituting equation (5) into (4) gives the equation for burning velocity as

$$S_u = \left(\frac{dr_i}{dt} \right) \left(\frac{r_i}{r_b} \right)^2 \left(\frac{P_i}{P} \right)^{1/\gamma_u} \quad (6)$$

but a relation is now needed between the pressure rise and the flame growth.

Equation (6) is as derived by Lewis and von Elbe.⁹ A temperature gradient is established in the burned gas region and the multizone model was developed, as



a before burning; b after burning

2 Position of elemental shell

reported in detail in Saeed and Stone.⁷ The final equations obtained, which incorporate the burned gas temperature gradient in the model, are given in the Appendix. The burning velocity in the present method is then calculated by utilising this multizone model and modifying the equation (6) as

$$S_u = \left(\frac{dp}{dt}\right) \left(\frac{dr_i}{dp}\right) \left(\frac{r_i}{r_b}\right)^2 \left(\frac{P_i}{P}\right)^{1/\gamma_u} \quad (7)$$

In equation (7) first term on the right hand side, dp/dt , is calculated from the experimental data file. The second term, dr_i/dp , is calculated from the multizone modelling program. Both r_i and r_b are functions of pressure, i.e.

$$r_i = f(p) \quad (8)$$

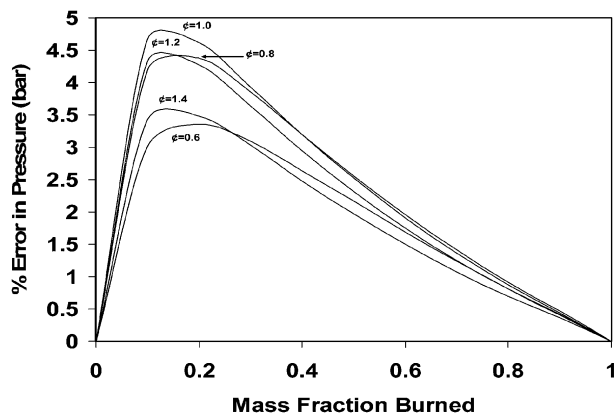
$$r_b = f(p) \quad (9)$$

$$x = \left(\frac{r_i}{R}\right)^3 \quad (10)$$

$$r_i = (x)^{1/3} R \quad (11)$$

But the burned gas volume and radius can be calculated from the following equations

$$v_b = V - m_i(n-1)(RuT_u/P) \quad (12)$$

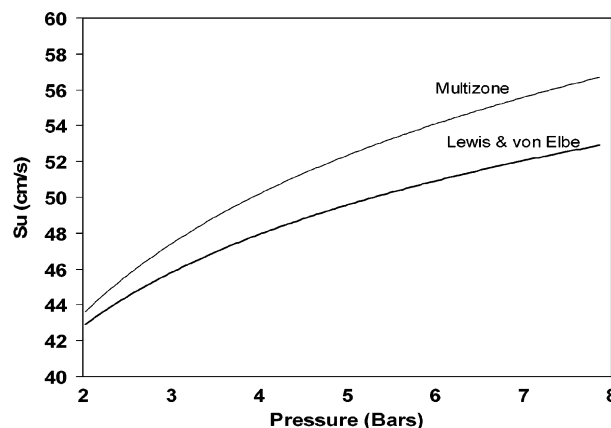


3 Variations of error in pressure with mass fraction burnt for propene-air mixtures in 10 zones model for initial conditions of 1 bar and 293 K

$$r_b = R[V - m_i(n-1)(RuT_u/P)]^{1/3} \quad (13)$$

Lewis and von Elbe⁹ assumed a linear relationship between the pressure rise and mass fraction burned. The multizone model shows that errors associated with the linear assumption peak at 0.1–0.2 mass fraction burned for any equivalence ratio. Figure 3 shows that for propene-air mixtures, the Lewis and von Elbe⁹ method would give an error of up to 5%, and the error is a maximum for a stoichiometric mixture. Figure 4 shows the burning velocity for propene-air mixtures as calculated from the Lewis and von Elbe⁹ method compared with the ten-zone burned gas model. Figure 4 shows that the percentage difference increases with the simultaneous increase in pressure and temperature.

The response of a flame to stretch is highly dependent on the Lewis number (Le), based on the deficient species. For mixtures with a Lewis number less than unity (highly diffusive reactants), increasing the stretch rate increases the flame temperature and there is an increase in the burning velocity according to Law.¹² Wu and Law¹³ investigated the effect of stretch on flames, and they showed that the effects of stretch at low stretch rates had minimal effects on the burning velocity results. In the spherical expanding flames, as in the present



4 Burning velocity as function of pressure and temperature as calculated from ten-zone model and Lewis and von Elbe method⁹ for stoichiometric, 293 K and 1 bar initial conditions

Table 1 Coefficients to be used in equation (14) for laminar burning velocity (m s^{-1}) of propene–air mixtures

Initial experimental temperature, K	$S_{u,0}$	$S_{u,1}$	$S_{u,2}$	$S_{u,3}$	$S_{u,4}$	α_0	β_0	α_1	β_1
1 293	0.3938	0.5370	-1.3897	-2.6339	3.8636	1.6599	-0.2279	0.0474	0.0505
2 425	0.3997	0.4306	-1.5167	-0.9965	2.1797	1.6500	-0.1641	0.7613	-0.2465
3 293+425	0.3999	0.4468	-1.5999	-1.6558	3.0971	1.6646	-0.2419	1.123	-0.0553

study, during the early stages of combustion the flame front has higher values of flame stretch due to the large curvature that is associated with a small spherical surface. As combustion proceeds, the radius of curvature increases and the flame stretch approaches zero asymptotically, and the ideal case of a 1D flame front is approached. In the present study, no corrections have been made for strain¹⁰ since only data from large flames (diameters greater than say 100 mm) have been used, and as combustion proceeds both the flame curvature decreases and the flame stretch falls to negligible values. This is in complete contrast to constant pressure spherical flame studies, which study the early growth of flames before there is any significant pressure rise. These flames by definition have small radii and high flame speeds (greater than the laminar burning velocity), and both factors give rise to high strain rates that cannot be ignored. Empirical justification for this is the good agreement of the current correlations with data from ambient conditions.³ The justification for ignoring the effects of buoyancy, the electrodes, and heat transfer is in Ref. 10. The range of equivalence ratio used is 0.8–1.6, with 0.1 steps. Tests were undertaken with initial temperatures of 293 K (25°C) and 425 K (152°C) and initial pressures of 0.5, 1.0, 2.0 and 3.5 bar.

The set of data obtained was fitted (using a least squares method) to the same form of correlation as used previously,¹⁰ to show the dependency of the laminar burning velocity on pressure, temperature and equivalence ratio

$$S_u = \quad (14)$$

$$\left[S_{u,0} + S_{u,1}(\phi - 1) + S_{u,2}(\phi - 1)^2 + S_{u,3}(\phi - 1)^3 + S_{u,4}(\phi - 1)^4 \right] \cdot [T^\alpha P^\beta]$$

where $S_{u,0}$, $S_{u,1}$, $S_{u,2}$, $S_{u,3}$, $S_{u,4}$, α_1 , β_1 , α_0 , β_0 are the coefficients, and

$$T = T_u/T_0 \text{ and } P = P_u/P_0$$

$$\alpha = \alpha_0 + (\phi - 1)\alpha_1 \text{ and } \beta = \beta_0 + (\phi - 1)\beta_1$$

Experimental results

Burning velocity as function of temperature and pressure

Two pressure–time experimental data sets with different initial temperatures were obtained for the propene–air mixtures. The first set of data was obtained for initial conditions of $T_1=293$ K, $P_1=0.5, 1, 2, 2.5$ and 3.5 bar, and for the range of equivalence ratio of 0.7 to 1.6 in the steps of 0.1. Similarly, the second set of experimental

data set was obtained for the range of initial conditions of $T_1=425$ K, $P_1=0.5, 1, 2.5$ and 3.5 bar, and equivalence ratios of 0.7 to 1.6 in the steps of 0.1. The laminar burning velocities were then determined from the above two sets of experimental data using the multizone model. Figure 5 shows a selection of plots of the laminar burning velocity along the unburned gas temperature isentropes, plotted against both temperature and pressure obtained for the above two data sets; the solid lines indicate the values obtained from the correlation.

The data were fitted with the correlation given in equation (14). The correlation fit was performed in three combinations:

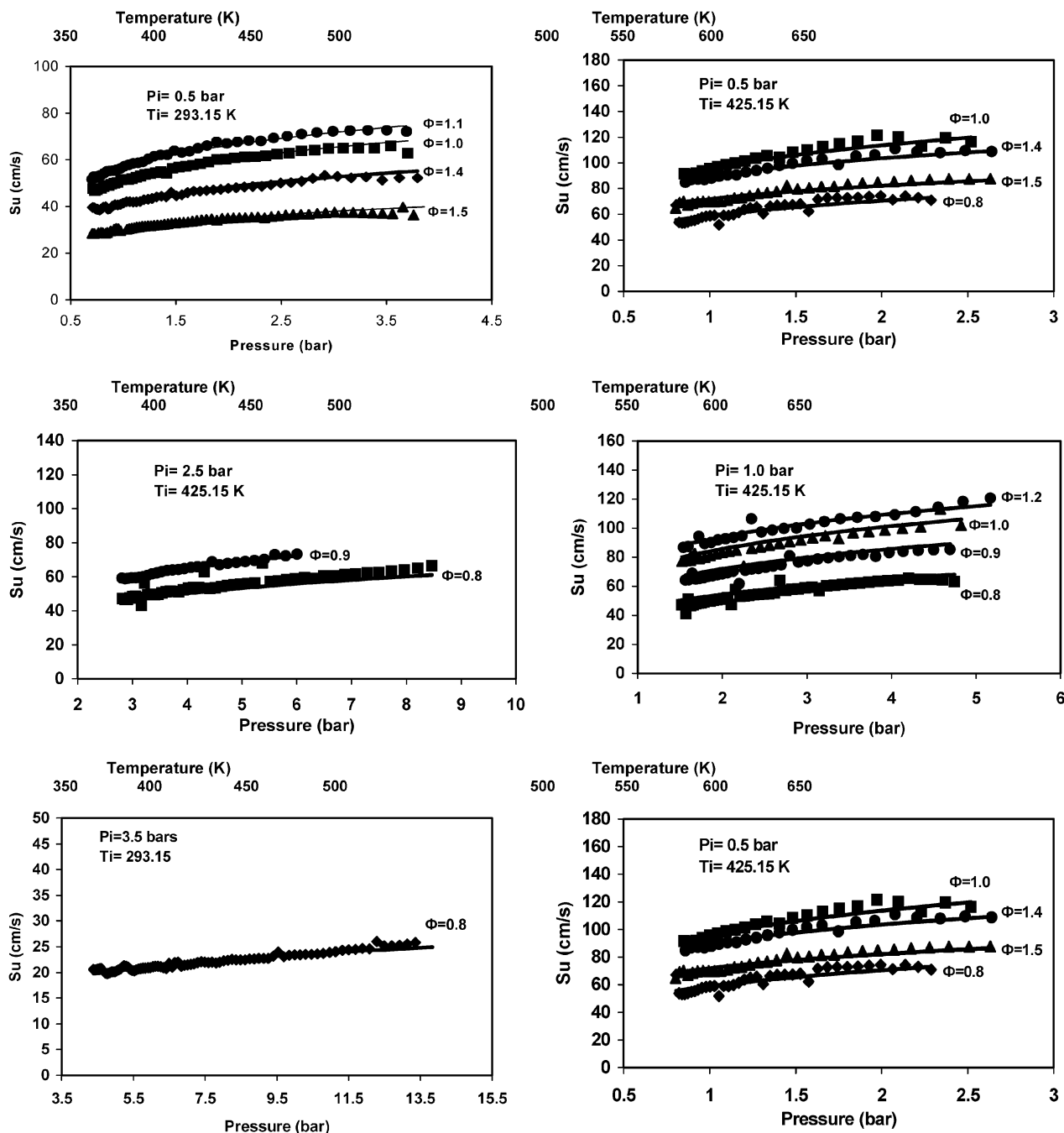
- using the data obtained from the first set of experiments (initial temperature of 293 K)
- using the data obtained from the second set of experiments (initial temperature of 425 K)
- for the combined data sets.

As a result, three sets of coefficients are shown in Table 1. In Table 1, first row shows the values of the coefficients obtained for the data set with an initial temperature of 293 K only (the ‘293 K correlation’), the second row shows the values of the coefficients obtained from the data sets with an initial temperature 425 K only (the ‘425 K correlation’), and the third row shows the values of the coefficients when the two data sets are combined. Table 2 shows a summary of the range of applicability for these coefficients. It can be seen from the Fig. 5 that the overall fit of the correlation with the experimental data is good and that the maximum difference between the experimental data and the correlation is found to be always less than 5% and mostly much smaller. The maximum deviation of the correlation fit and the experimental data are observed in the later stages of combustion at elevated temperatures and pressures. This could be due to the inclusion of some cellular flame data as an indirect method for the elimination of cellular data points was used; this is discussed later.

Figure 6 shows a comparison of the burning velocities obtained by using the three different coefficient sets given in Table 1 with equation (14). The comparison is made for the burning velocities obtained from the three correlations at conditions of *a* 293 K and 1 bar, and *b* 425 K and 1 bar. This is a severe test of the correlations, since in Fig 6*a* the low temperature data (initial 293 K) have been extrapolated up to 425 K, and in Fig 6*b* the high temperature data (initial 425 K) have been extrapolated down to 293 K. It can be seen in Fig 6*b* that the values obtained from the three correlations give a good

Table 2 Range of validity for correlation coefficients in first, second and third rows of Table 1

Initial experimental temperature, K	P , bar	T , K	Equivalence ratio	Burning velocity, cm s^{-1}
1 293	0.5–13.5	295–500	0.7–1.5	>10
2 425	0.5–8.5	425–650	0.9–1.5	>20
3 293+425	0.5–13.5	295–650	0.9–1.5	>10



5 Variation of laminar burning velocity as function of pressure and temperature for data obtained along isentrope; solid line indicates correlation fit using equation (1)

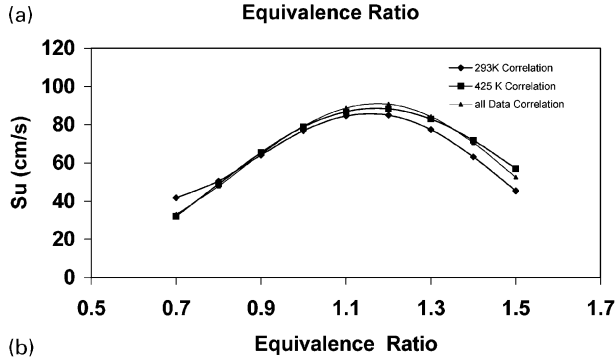
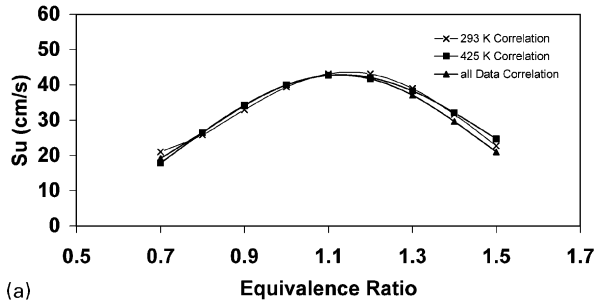
agreement. In Fig 6a it can be seen that the values obtained from the three correlations give a good agreement on the lean side but the ‘425 K’ and ‘all data’ correlations give higher burning velocities than those obtained from the ‘293 K’ correlation.

Burning velocity as function of equivalence ratio

Figure 7 shows a comparison of the laminar burning speed of propene-air mixtures obtained in the present study with that of the earlier reported data. A comparison is made with the data of Gibbs and Calcote⁶ and Günther and Janisch¹⁴ (who used a Bunsen burner technique), Gerstein *et al.*⁵ (who used flame propagation in a tube), Davis and Law³ (who used a counter flow flame technique that is now well established), and Jomaas *et al.*⁴ (who used a high pressure constant

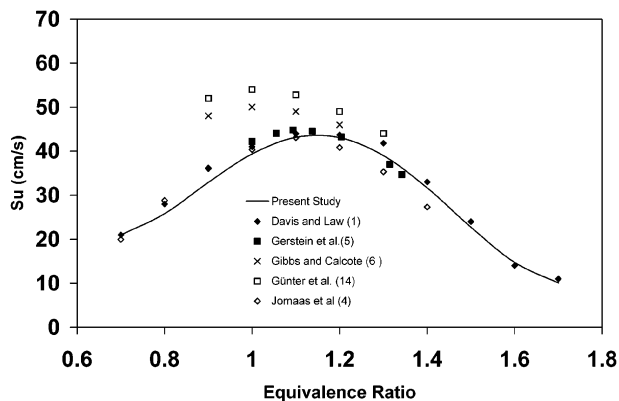
volume cylindrical test facility). It can be seen from Fig 7 that the peak in burning velocity is obtained for $\phi=1.1$, and that there is a good agreement in burning velocity data obtained from the present study with the data of Gerstein *et al.*⁵ and Davis and Law.³

The maximum burning velocity obtained from the present study is 43.1 cm s^{-1} at $\phi=1.1$. At the same equivalence ratio, Gerstein *et al.*⁵ and Davis and Law³ have reported the maximum burning velocity as 43.8 and 44 cm s^{-1} respectively. The agreement with the most recent data of Jomaas *et al.*⁴ is good for weak and stoichiometric mixtures, but less good for the rich mixtures. For rich mixtures there is a difference of $\sim 5 \text{ cm s}^{-1}$ in the data between the counterflow flame technique data of Davis and Law³ and the most recent data of Jomaas *et al.*⁴ using the high pressure constant

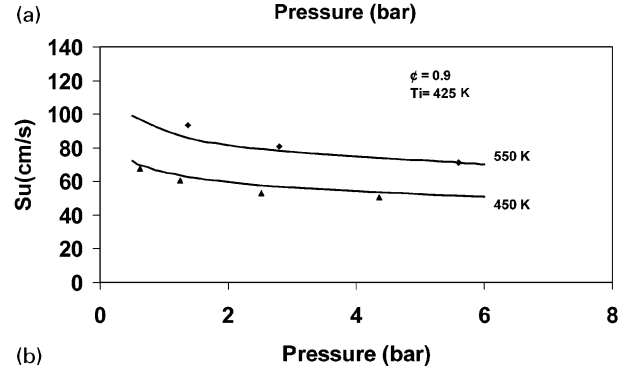
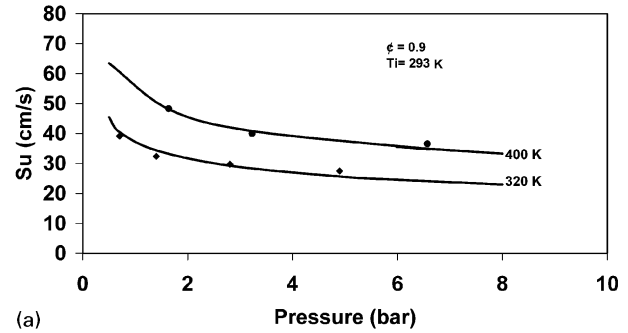


6 Comparison of burning velocities at *a* 293 K and 1 bar and *b* 425 K and 1 bar obtained from three sets of correlation coefficients

pressure facility. Although Jomaas *et al.*⁴ presents both sets of data, there are no comments as to the discrepancy with their earlier data in Davis and Law.³ Jomaas *et al.*⁴ used the high pressure constant pressure facility developed and explained in Tse *et al.*¹⁵ and Rozenchan *et al.*,¹⁶ which is an ingenious system, with a vented cylindrical chamber within a larger cylindrical vessel that provides a buffer volume. Initially the flame will be spherical, and although its cross-section will be circular it will not remain spherical, and nor is the gas free to flow radially in the central plane. The correction for the effects of strain by Jomaas *et al.*⁴ assumes the flame to be growing spherically, so only flame growth until its diameter is about half that of the inner chamber are used. Scatter in the data at 2 and 5 atm makes a comparison with the correlations reported here difficult. It is seen that for all ranges of equivalence ratios the difference in the burning velocity data is no more than 2 cm s^{-1} . However, this is in substantial disagreement with the data of Gibbs and Calcote⁵ and Günther and Janisch.¹⁴ The difference is as large as $10\text{--}15 \text{ cm s}^{-1}$, which can be attributed to the



7 Comparison of laminar burning velocity from current correlation with that of earlier reported data at 1 bar and 298 K



8 Effect of pressure on burning velocity of propene-air mixtures: solid lines indicate correlation fit for equivalence ratio of 0.9 and initial pressure of 1 bar and temperatures of *a* 298 and *b* 425 K

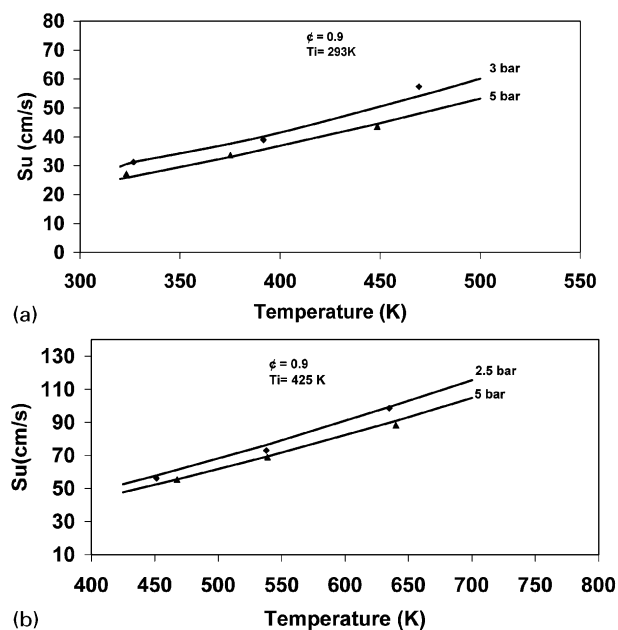
errors associated with presence of high flame stretch, to burner technique related errors such as the significant changes in the velocity distribution beside the burner rim, with divergence of the flow lines, flame area measurement, entrainment of the air into the flame cone base, and heat transfer to the burner tube.

Burning velocity as function of pressure

Figure 8 shows the dependence of the burning velocity on the pressure at a fixed unburned gas temperature. The experimental data points are at fixed equivalence ratio of 0.9 and unburned temperatures of 320, 400, 450 and 550 K but varying pressures (a consequence of the different initial pressures). For the experimental data points of 320 and 400 K, the '293 K' correlation is used and for the data points of 450 and 550 K, the '425 K' correlation is used. It can be seen that the burning velocity decreases with increasing pressure and the correlation gives a very good fit to the experimental data points. However, there is some underestimation for the range of 1–2 bar in Fig. 8*a* at the fixed unburned gas temperature of 550 K. This may be because the experimental data points for 550 K lie at the final stages of combustion, which might be affected by heat transfer to the wall from the flame front. For all other points the correlation gives a very good agreement with the experimental data points. Figure 8 uses data for the 0.9 equivalence ratio not stoichiometric, since cellularity was found to trigger earlier with high pressure stoichiometric mixtures.

Burning velocity as function of temperature

The burning velocity is found to increase with increasing temperature. Figure 9 shows the dependence of the burning velocity on unburned gas temperature with pressure as a fixed parameter. Figure 9*a* shows the variation of the burning velocity as a function of temperature

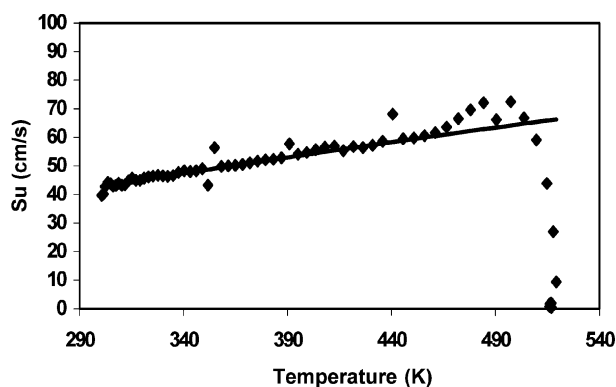


9 Effect of temperature on burning velocity of propene-air mixtures: solid lines indicate correlation fit for equivalence ratio of 0.9, initial pressure of 1 bar and temperatures of a 298 and b 425 K

for pressures of 3 and 5 bar, using data from experiments with different initial pressures. The experimental data points shown are for an equivalence ratio of 0.9 and an initial temperature of 293 K; the line shows the values obtained using the 293 K correlation. Similarly, Fig. 9b shows the variation of the burning velocity as a function of temperature for fixed pressures of 2.5 and 5 bar. The experimental data points shown are for an equivalence ratio of 0.9 and initial fixed temperature of 425 K, and the line shows the '425 K' correlation fit. It can be seen from Fig. 9a and b that there is a good agreement between the experimental data points and the correlations.

Cellular flames

Investigators using the constant volume method for the determination of the burning velocities have in the past often assumed that the flame front is smooth, and there is no cellularity or wrinkling of the flames. However, theoretical and experimental studies, for example Markstein,¹⁷ Joulin and Clavin,¹⁸ Zeldovich,¹⁹ Groff²⁰ and Bradley *et al.*²¹ observed that flames, particularly in rich hydrocarbon mixtures at high pressures, are conducive to the development of, first a 'crack line', then a cellular flame structure. This flame instability is attributed to both hydrodynamic and thermodynamic effects, and concerns a smooth, stable propagating flame becoming unstable, and then creating at smaller wavelengths a stable structure comprised of different size cells in dynamic equilibrium, which later become unstable. In the present analysis, the flame front is assumed to be smooth and spherical. However, the transformation of the smooth flame front to that of the polyhedral-cellular flames causes an increase in the surface area, and the temperature, so the validity of the assumption of a smooth flame is violated. The burning velocity is observed to increase because of the increased surface area of the flame front. Figure 10 shows how this leads to a sudden increase in the burning velocity and a departure from the value predicted by the correlation



10 Formation of cellular flames in stoichiometric propene-air mixture for initial condition of 293 K and 1 bar

(solid line). Cellularity was found to exist for some propene-air mixtures and the vertical lines in Fig. 11 indicate its possible start. No discontinuity in the burning velocity was found with a 0.5 bar initial pressure and initial temperatures of 293 and 425 K for any equivalence ratio. An appreciable rise in burning velocity was observed along the isentrope for initial conditions of 1, 2 and 3.5 bar, and initial temperatures of both 293 and 425 K. The onset of cellularity is earlier with an increase in initial pressure; the conditions for the onset of cellularity are given in Table 3.

Conclusions

A multizone model has been used to study the combustion of propene with air inside a closed vessel so as to determine the laminar burning velocities at varying equivalence ratios, temperatures and pressures.

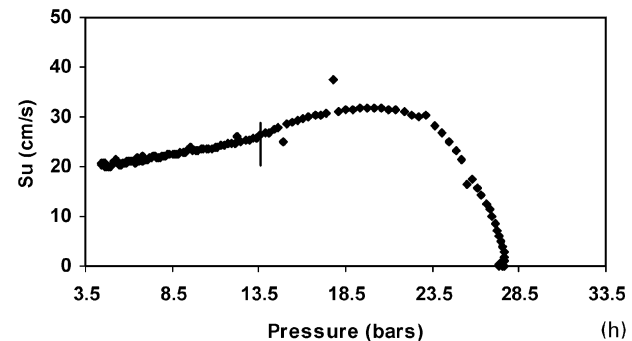
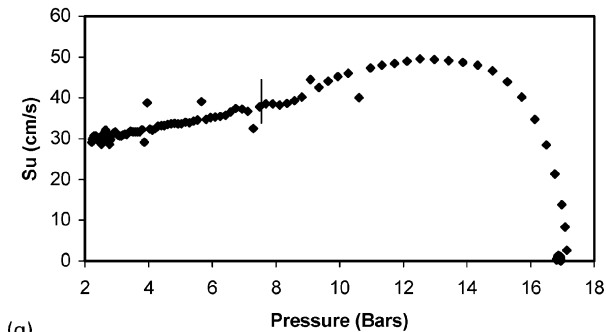
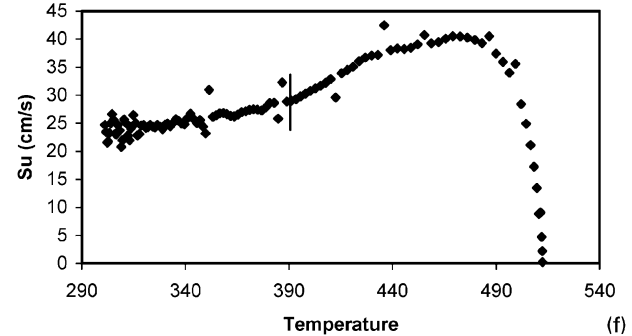
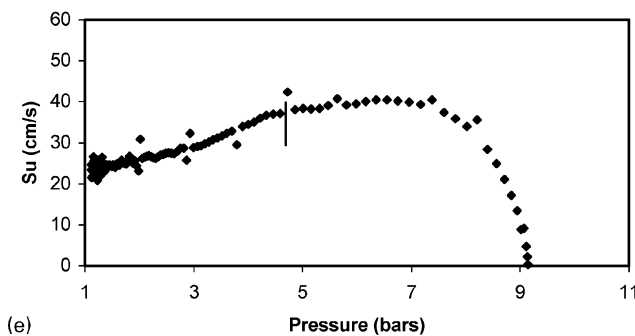
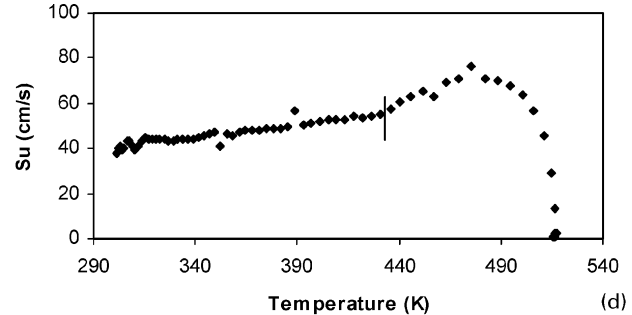
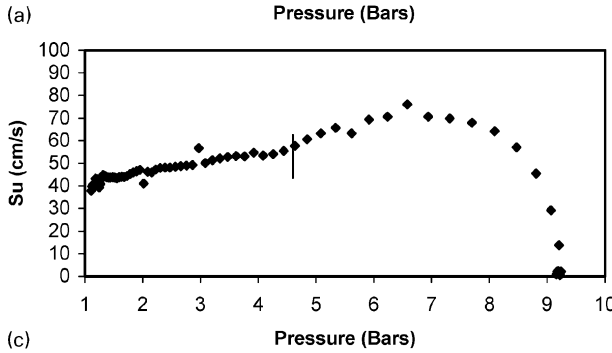
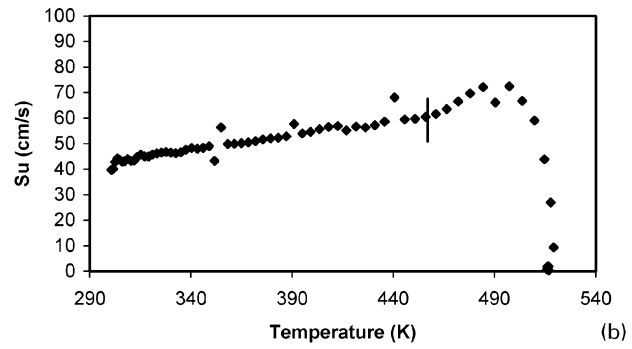
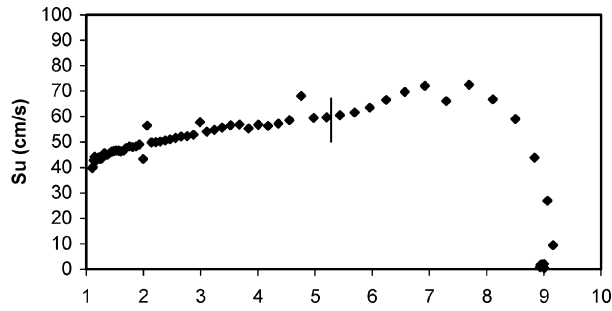
1. The relationship between the fractional pressure rise and the mass fraction burned is non-linear for propene. The errors associated with the linear assumption peak at 0.1–0.2 mass fraction burned for all the equivalence ratios burned. The maximum error (~5%) is found to be for stoichiometric mixtures.

2. The temperature gradient in the burned gas has an effect on the end pressure for propene and if this is ignored the error can be as large as 5%.

3. The multizone burning velocity technique has been used for the determination of the laminar burning velocities of propene-air mixtures at varying equivalence ratios, temperatures and pressures.

Table 3 Temperature, pressure and time at onset of cellular flames

T_i , K	P_i , bar	Phi	t_c , ms	T_c , K	P_c , bar
293	1.0	1.1	32.4	466	5.95
293	1.0	1.2	30.8	458	5.59
293	1.0	1.3	30.4	427	4.25
293	1.0	1.4	34.8	395	3.15
293	1.0	1.5	43.6	377	2.64
293	2.0	0.9	46.4	428	8.34
293	2.0	1.0	34.4	391	5.96
293	3.5	1.0	70.8	414	12.6
293	3.5	0.8	37.6	349	6.72
425	1.0	1.2	23.2	617	4.55
425	1.0	1.3	22.8	591	3.84
425	1.0	1.4	24.0	559	2.93
425	1.0	1.5	29.6	539	2.65
425	2.0	0.9	30.0	562	6.01
425	2.0	1.0	21.2	501	3.79



a $\Phi=1.1$, $P_i=1.0$ bar, $T_i=293.15$ K; b $\Phi=1.1$, $P_i=1.0$ bar, $T_i=293.15$ K; c $\Phi=1.3$, $P_i=1.0$ bar, $T_i=293.15$ K; d $\Phi=1.3$, $P_i=1.0$ bar, $T_i=293.15$ K; e $\Phi=1.5$, $P_i=1.0$ bar, $T_i=293.15$ K; f $\Phi=1.5$, $P_i=1.0$ bar, $T_i=293.15$ K; g $\Phi=0.9$, $P_i=2.0$ bar, $T_i=293.15$ K; h $\Phi=0.8$, $P_i=3.5$ bar, $T_i=293.15$ K

11 Conditions which led to formation of cellular flames in spherical vessel with propene-air mixtures

4. The burning velocity for propene-air mixtures compares well with the earlier reported data at ambient conditions by Davis and Law.³ The current data are the only ones known for high temperatures and pressures.

5. Cellular flames were found to occur in some test runs, and the conditions at the onset of cellularity have been tabulated.

Appendix

Multizone model

For a constant volume encasing the rigid adiabatic spherical close vessel a differential form of conservation equation is given as

$$m \frac{de}{dt} - \frac{dQ}{dt} = 0 \tag{15}$$

At any instant of time during combustion, the contents of the closed vessel consist of the burned and the unburned gases separated by the flame front of zero thickness. The equation for the conservation of volume and internal energy are given by the equations (16) and (17)

$$v = V/M = xv_b(P, T_b) + (1-x)v_u(P, S_{u,o}) \tag{16}$$

$$e = E/M = xe_b(P, T_b) + (1-x)e_u(P, S_{u,o}) \tag{17}$$

The above three equations are solved as a set of ordinary differential equations for the rate of change of pressure,

burned and unburned gas temperatures for a single burned zone. These differential equations can be extended to multiple burned gas zones for the multizone analysis. For the multizone analysis with N zones, there will be $N+3$ equations to be solved simultaneously. The extension of the single burned gas zone to multiple zones is as follows

$$\frac{dP}{dt} = \frac{A + B_u + \Sigma B_i}{\Sigma C_i + D} \quad (18)$$

$$\frac{dT_u}{dt} = \frac{-h\left(\pi \frac{b^2}{2} + \frac{4V}{b}\right)(1-x^{0.5})(T_u - T_w)}{m(1-x)C_{p,u}} + \frac{v_u}{C_{p,u}} \frac{\partial \ln v_u}{\partial \ln T} \left(\frac{A + B_u + \Sigma B_i}{\Sigma C_i + D} \right) \quad (19)$$

$$\begin{aligned} \frac{dT_{bi}}{dt} = & -(1-x) \frac{v_u}{T_u} \frac{\partial \ln v_u}{\partial \ln T_u} \cdot \frac{T_{bi}}{xv_{bi}} \frac{\partial \ln T_{bi}}{\partial \ln v_{bi}} \\ & \frac{v_u}{C_{p,u}} \frac{\partial \ln v_u}{\partial \ln T_u} \cdot \frac{\partial \ln v_u}{\partial \ln T_u} \left(\frac{A + B_u + \Sigma B_i}{\Sigma C_i + D} \right) + \\ & \frac{v_u}{T_u} \frac{\partial \ln v_u}{\partial \ln T} \cdot \frac{T_{bi}}{xv_{bi}} \frac{\partial \ln T_{bi}}{\partial \ln v_{bi}} \cdot \frac{hA(1-x^{0.5})(T_u - T_w)}{mC_{p,u}} - \\ & \frac{T_{bi}}{xv_{bi}} \frac{\partial \ln T_{bi}}{\partial \ln v_{bi}} \left[x \frac{v_{bi}}{P} \frac{\partial \ln v_{bi}}{\partial \ln P} + (1-x) \frac{v_u}{P} \frac{\partial \ln v_u}{\partial \ln P} \right] \\ & \left(\frac{A + B_u + \Sigma B_i}{\Sigma C_i + D} \right) - \frac{T_{bi}}{xv_{bi}} \frac{\partial \ln T_{bi}}{\partial \ln v_{bi}} (v_{bi} - v_u) \frac{dx}{dt} \end{aligned} \quad (20)$$

where, $\Sigma(B_i) = B_1 + B_2 + B_3 + \dots + B_n$

$$A = \frac{v_u}{C_{p,u}} \frac{\partial \ln v_u}{\partial \ln T_u} \cdot hA(1-x^{0.5}) \frac{(T_u - T_w)}{T_u} \quad (21)$$

$$B_u = (v_u - h_u) \frac{dx}{dt} \quad (22)$$

$$B_i = \left(-v_{bi} + \frac{v_{bi}}{C_{p,bi}} h_{bi} \right) \frac{dx}{dt} \quad (23)$$

$$C_i = x \left[\frac{v_{bi}^2}{C_{p,bi} T_{bi}} \left(\frac{\partial \ln v_{bi}}{\partial \ln T_{bi}} \right)^2 + \frac{v_{bi}}{P} \frac{\partial \ln v_{bi}}{\partial \ln P} \right] \quad (24)$$

$$D = (1-x) \left[\frac{v_u^2}{C_{p,u} T_u} \left(\frac{\partial \ln v_u}{\partial \ln T_u} \right)^2 + \frac{v_u}{P} \frac{\partial \ln v_u}{\partial \ln P} \right] \quad (25)$$

References

1. I. Glassman: 'Combustion'; 1996, London, Academic Press.
2. S. G. Davis, C. K. Law and H. I. Wang: *Combust. Flame*, 1999, **119**, 375-399.
3. S. G. Davis and C. K. Law: *Combust. Sci. Technol.*, 1998, **140**, 427-449.
4. G. Jomaas, X. L. Zheng, D. L. Zhu and C. K. Law: *Proc. Comb. Inst.*, 2005, **30**, 193-209
5. M. Gerstein, O. Levine and E. L. Wong: *J. Am. Chem. Soc.*, 1951, **73**, 418-422.
6. G. J. Gibbs and H. F. Calcote: *J. Chem. Eng. Data*, 1959, **4**, 226-237.
7. K. Saeed and C. R. Stone: *Combust. Flame*, 2004, **139**, (1-2), 152-166.
8. K. Saeed and C. R. Stone: *Combust. Theory Modell.*, 2004, **8**, (4), 721-743.
9. B. Lewis and G. von Elbe: *J. Chem. Phys.*, 1934, **2**, 283-290.
10. R. Stone, A. Clarke and P. Beckwith: *Combust. Flame*, 1998, **114**, 546-555.
11. M. Metghalchi and J. C. Keck: *Combust. Flame*, 1980, **38**, 143-154.
12. C. K. Law: *Proc. Comb. Inst.*, 1998, **22**, 1381-1402.
13. C. K. Wu and C. K. Law: *Proc. Comb. Inst.*, 1984, **20**, 1941-1949.
14. R. Günther and G. Janisch: *Chem. Ing. Technol.*, 1971, **43**, 975-978.
15. S. D. Tse, D. Zhu and C. K. Law: *Rev. Sci. Instr.*, 2004, **75**, (1) 233-239.
16. G. Rozenchan, D. L. Zhu, C. K. Law and S. D. Tse: *Proc. Comb. Inst.*, 2002, **29**, 1461-1469.
17. G. H. Markstein: 'Nonsteady flame propagation'; 1964, London, Pergamon Press.
18. G. Joulin and P. Clavin: *Combust. Flame*, 1979, **35**, 139-139.
19. Y. B. Zeldovich: *Combust. Flame*, 1981, **40**, 225.
20. E. G. Groff: *Combust. Flame*, 1982, **48**, 51-62.
21. D. Bradley, C. G. W. Sheppard, R. Woolley, D. H. Greenhalgh and R. D. Lockett: *Combust. Flame*, 1976, **122**, 195-217.

Authors Queries

Journal: **Journal of the Energy Institute**

Paper: **9332**

Title: **Laminar burning velocities of propene–air mixtures at elevated temperatures and pressures**

Dear Author

During the preparation of your manuscript for publication, the questions listed below have arisen. Please attend to these matters and return this form with your proof. Many thanks for your assistance

Query Reference	Query	Remarks
1	Author: please confirm the short title.	